

Study of the mechanism of steel cutting with the weakly focused radiation from a repetitively pulsed CO₂ laser

G G Gladush, S V Drobyazko, N B Rodionov, L I Antonova, Yu M Senatorov

Abstract. A study was made of the process of steel plate cutting with a weakly focused radiation from a repetitively pulsed CO₂ laser with the output of no more than 500 W without the use of a gas jet. The regimes were determined in which the removal of the melt under the action of the vapour recoil momentum proved to be more efficient than the melt removal under continuous irradiation. The physical mechanism of the process was proposed and its numerical model was elaborated. A comparison with experiments showed that this model provides a qualitatively adequate description of the experimental data and that it can be employed for the evaluation of remote cutting with high-power laser radiation.

1. Introduction

The use of a CO₂ laser with an output power of ~ 50 kW for remote cutting of metal structures ~ 50 m away from the laser or more was proposed in Ref. [1]. Cutting under these conditions differs from the conventional gas-laser cutting by the absence of an additional gas jet and a weak focusing of the laser radiation because of the long distance to the object. These specific features of remote laser cutting lower its efficiency because the removal of a melted material is hindered in this case. Indeed, the melt is usually ejected from the interaction region by either the gas jet or due to the vapour recoil pressure.

It was shown in Ref. [2] that upon the remote cutting of vertically mounted plates by the radiation from a horizontally moving cw CO₂ laser the melt can flow out, under certain conditions, by gravity. However, the melt region has to be wide for the material to be removed in this way, which makes this cutting mechanism inefficient [3]. To enhance the mass transfer, the modulation of laser radiation was proposed [1]. For a high off-duty ratio, the pulse intensity of even a weakly focused laser radiation is indeed high enough to provide the transient boiling of the metal surface and the required vapour recoil pressure. It remains unclear under

what circumstances this additional mass transfer compensates for the expenditures of energy for vaporisation and what the efficiency of this process is. The aim of this work is to investigate these questions.

2. Formulation of the problem

The mass removal upon single-pulse laser irradiation, when the depth of the melted region is far less than its width and the plate thickness, has been adequately studied to date (see papers [4, 5] and references therein). Because a single pulse cannot destroy the surface of a steel plate in our experiments, of prime importance is heating of the interaction region to the melting temperature, which is followed by the surface destruction.

Therefore, the cutting procedure in our case cannot be represented as a simple summation of the events of material ejection driven by single pulses. Because the mass transfer in this case is occurs at the high average heating temperature of the interaction region, along with the above-mentioned melt removal under the action of vapour, other mechanisms are also possible. When the plate is melt through, the recoil pressure can force out the melt forward in the beam direction. And, finally, the melt can simply flow out by gravity [3].

There exist papers (see, e. g., Refs [4, 5]) concerned with the drilling and cutting of metals with the radiation from a repetitively pulsed laser. Gas jets also were not employed in these papers, but the processing was performed by a tightly focused radiation, provided a single pulse could destroy the metal surface. In this case, the radiation intensity was more than an order of magnitude higher than that used in our work. The weld seam or the blind cut took the so-called shape of a dagger, which is qualitatively different from our case.

3. Experimental procedure and measuring technique

The laser beam passed through a KCl plate mounted at an angle of 45° to the beam direction and was focused with a lens on a vertical metal plate fixed on the table of a milling machine, which ensured a horizontal target translation with a velocity ranging from 2.5 to 1600 mm min⁻¹. A part of the radiation ($\sim 4\%$ of the energy) was directed by a KCl plate to an IMO-2N power meter. The dimension of the spot on the target was determined by the focal length of the lens and was adjusted by its displacement. The parameters of the laser setup are given below:

G G Gladush, S V Drobyazko, N B Rodionov, L I Antonova, Yu M Senatorov
State Scientific Centre of the Russian Federation 'Troitsk Institute for
Innovation and Fusion Research', 142092 Troitsk, Moscow oblast, Russia

Received 16 June 2000

Kvantovaya Elektronika 30 (12) 1072–1076 (2000)

Translated by E N Ragozin

Average output power \bar{P} 1 kW
 Pulse repetition rate f 0.1–200 Hz
 Pulse duration (at the 0.1 maximum) τ 20–500 μ s
 Pulse energy E_i 0.1–8 J
 Diameter of the output beam d_f 45 mm

The pulse duration was measured with a photodetector cooled to liquid nitrogen temperature. The distribution of laser energy in the focal spot had the shape of a frustum of a cone with a steep drop at the edges. The intensity modulation of the flat portion of the distribution amounted to $\sim 20\%$. The pulse repetition rate and the number N of pulses in a train could be varied during experiments. The absorption coefficient of the target averaged over the train was determined by measuring sample temperature with a chromel-alumel thermocouple during pulsed irradiation. Specific volume energy expenditures were defined as the ratio $X = E_i N / v$ between the total laser energy $E_f = E_i N$ in the train and the volume v of the removed material.

4. Experimental results

Cutting of steel plates under our experimental conditions is always accompanied by the appearance of a plasma plume. The radiation intensity that produces the optical breakdown at the target decreases slowly as the focal spot area increases and approaches a threshold intensity of $(1 - 2) \times 10^5 \text{ W cm}^{-2}$ measured in Ref. [6] for very large irradiation areas.

Fig. 1 shows the appearance of the cuts of a steel plate of thickness h made under different conditions. The cut widths d_c are always 2–3 times smaller than the focal spot dimension. Ridges of solidified melt are seen at the cut edges. The upper and lower ridges (for a vertical plate mount) are identical. Cutting for a sample translation upwards or downwards is similar to cutting for its horizontal translation. The value of d_c decreases monotonically as the cutting speed V increases (see Table 1). On reaching the critical speed, the

cut width drops to zero in a jump-like manner – cutting gives way to welding. As a rule, the plate is fused through in this case. A deepening is observed on the front side, while the rear side remains slightly perturbed. This transition is often accompanied by the appearance of a number of holes (see Fig. 1).

Table 1. Dependence of the cut width d_c on the experimental conditions for $d_f = 3 \text{ mm}$, $h = 0.5 \text{ mm}$, and $f = 100 \text{ Hz}$.

| \bar{P}/W | $\tau/\mu\text{s}$ | $V/\text{mm s}^{-1}$ | $X/\text{kJ cm}^{-3}$ | $d_c \text{ (MM)}$ | |
|--------------------|--------------------|----------------------|-----------------------|--------------------|-------------|
| | | | | experiment | calculation |
| 380 | 70 | 0.5 | 250 | 2.2 | 2.3 |
| | | 1.0 | 100 | 2.0 | 2.3 |
| | | 2.5 | 80 | 1.5 | 1.5 |
| 280 | 70 | 0.6 | 240 | 1.8 | 1.5 |
| | | 1.0 | 170 | 1.4 | 1.5 |
| | | 2.5 | 150 | 0.9 | 1.5 |
| 280 | 150 | 1.0 | 400 | 1.3 | 2.2 |
| | | 2.0 | 200 | 1.1 | 1.5 |
| | | 4.0 | 150 | 0.6 | 1.0 |

In practice, the cut width is usually not important, and the critical cutting speed V_{cr} is a more important parameter. Fig. 2 shows this speed as a function of the laser radiation power. As expected, the critical speed rises with the average radiation power. The average radiation power was changed either by varying the pulse energy for an invariable repetition rate or by varying the pulse repetition rate for a constant pulse energy. One can see that the critical speed depends only slightly on the features of the procedure, being primarily determined by the average laser power. This is additionally confirmed by the fact that V_{cr} is independent of the focal spot dimension for a constant average laser power ($f = 100 \text{ Hz}$, $E_i = 3.2 \text{ J}$, $\tau = 70 \mu\text{s}$). The focal spot dimension was varied from 3.8 to 1.7 mm; in this case, the average cut width also narrowed by about a factor of two.

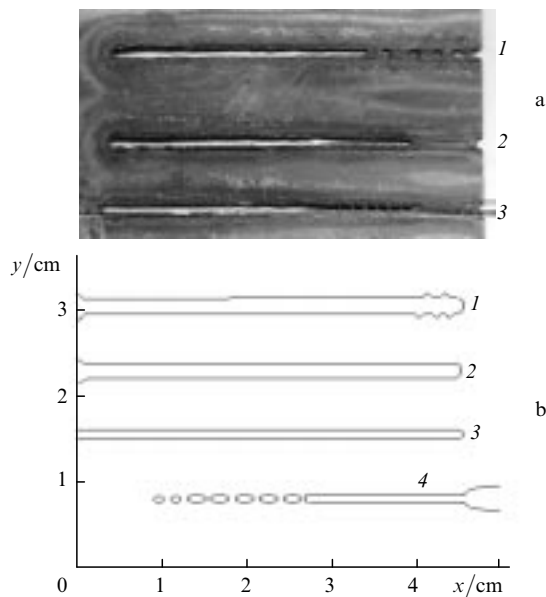


Figure 1. Appearance of experimental (a) and theoretical (b) cuts. The experiment was conducted for $d_f = 3 \text{ mm}$, $f = 100 \text{ Hz}$, $\tau = 70 \mu\text{s}$, and $\bar{P} = 370 \text{ (1)}$, 280 (2) , and 235 W (3) . The calculations were performed for $\bar{P} = 380 \text{ (1 - 3)}$ and 310 W (4) , $V = 0.4 \text{ (1)}$, 1 (2) , 2 (3) , and $6 \text{ mm s}^{-1} \text{ (4)}$. The coordinate axes coincide with the plate edges.

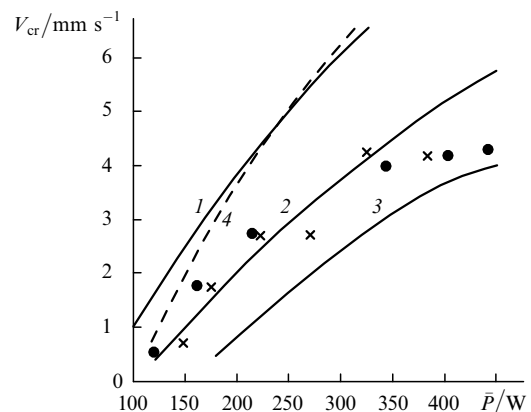


Figure 2. Experimental (symbols) and calculated (curves) dependences of the critical cutting speed on the average laser power for $f = 100 \text{ Hz}$, $\tau = 70 \mu\text{s}$, $d_f = 3 \text{ mm}$ (\times); $E_i = 2.2 \text{ J}$, $\tau = 70 \mu\text{s}$, $d_f = 3 \text{ mm}$ (\bullet); $f = 100 \text{ Hz}$ ($1 - 3$), the absorption coefficient for the laser radiation $\alpha = 30\%$ (1), 20% (2), and 15% (3); $E_i = 2.2 \text{ J}$, $\alpha = 30\%$ (4).

The specific energy of cutting as a function of the plate translation velocity is presented in Table 1. One can see

that this energy is, if the absorption is taken into account, significantly lower than the specific evaporation energy of steel (65 kJ cm⁻³). This fact suggests that the removal of material in remote cutting is caused not only by the material evaporation alone. Before discussing the experimental results, it is reasonable to consider the mechanism of the process, its model, and the results of numerical calculations based on this model.

5. Numerical model

In a repetitively pulsed irradiation regime with a high off-duty ratio, the temperature distribution and the shape of the cut in a moving metal plate are three-dimensional and transient. For an infinite continuous plate moving with a constant velocity, the temperature distribution is represented in the form of series [5]. However, the plate is not continuous upon cutting, its temperature field being significantly distorted owing to the presence of the cut. A part of the radiation passes through the cut and is lost. Typically, only a part of the plate surface in the focal spot boils up, and therefore the surface source of plate heating can have a complex profile, which is different from a Gaussian usually assumed in the derivation of the analytic expression [5].

The numerical computational model is free from these drawbacks but is rather complex, being three-dimensional. To simplify the problem, one can use several circumstances. Because of a short duration of the radiation pulse, the temperature distribution can be represented as a sum of two functions: the slow one \bar{T} and the fast one δT . The temperature δT strongly fluctuates in a thin near-surface layer, and therefore we can treat this heating as one-dimensional and analyse it analytically [5].

The average temperature \bar{T} changes under exposure to a large number of pulses and is determined from the balance between the average radiation power and the heat removal by thermal conduction and sample translation. Because the temperature \bar{T} varies slowly and is smoothly distributed along the surface, and the plate has a small thickness, the plate can be treated as thermally thin. Therefore, \bar{T} will be determined from the solution of the heat conduction equation, as in the case of cutting by cw radiation [3]:

$$c \frac{\partial \bar{T}}{\partial t} - \lambda \left(\frac{\partial^2 \bar{T}}{\partial x^2} + \frac{\partial^2 \bar{T}}{\partial y^2} \right) = \alpha \frac{\bar{q}}{h} \exp \left[-\frac{(x - Vt)^2 + y^2}{r_f^2} \right] - \frac{\varepsilon \sigma}{h} \bar{T}^4 - \frac{q_e}{h} \theta(T_b - \bar{T}) - \frac{q_c}{h}, \quad (1)$$

where c and λ are the heat capacity and the thermal conductivity coefficient; \bar{q} and α are the average intensity and the absorption coefficient of laser radiation; V and r_f are the velocity of motion of the light spot and its radius; σ is the Stefan—Boltzmann constant; ε is the thermal emissivity; θ is the Heaviside function; and T_b is the boiling temperature of the plate material. The last three terms in the right-hand side of Eqn (1) describe the losses by the thermal radiation from the surface, the heat losses by evaporation q_e , and by natural air convection q_c . The last two processes will be described in the simplest way, because a qualitative description is sufficient in our case [3]:

$$q_e = \frac{2.56 \cdot 10^3}{\sqrt{\bar{T}}} (p_s - p_0), \quad p_0 = 760.$$

The saturation vapour pressure p_s (iron is assumed to be under cutting) is described by the expression [5]

$$p_s = \frac{4 \cdot 10^{13.27 - 19710/\bar{T}}}{\bar{T}^{1.27}}.$$

In these expressions, the pressure is expressed in mm Hg and the temperature in Kelvins. The expression for convective cooling was borrowed from Ref. [7]:

$$q_c = \lambda_a \frac{\bar{T} - \bar{T}_a}{H^{1/4}} \left(\frac{g}{v^2} \right)^{1/4},$$

where λ_a and v are the thermal conductivity and kinematic viscosity coefficients of air; H is the characteristic vertical dimension of the sample; \bar{T}_a is the ambient air temperature; and g is the free fall acceleration.

We will use the boundary condition of the second kind to the plate edges and the cut. Because these boundaries are free, $\partial \bar{T} / \partial \mathbf{n} = 0$, where \mathbf{n} is the normal to the boundaries. The initial condition has the form $\bar{T} = \bar{T}_a$. To simplify the calculations in Eqn (1), the phase transition energy in the melting of a material (for iron, it does not exceed 30% of the heat content at the melting temperature) is not taken into account, as is customary with problems on laser technology. For the same reason the thermal constants were assumed to be invariable and close to those of the 'st.3' steel ($\lambda = 0.3$ W cm⁻¹ K⁻¹, $\lambda/c = 0.13$ cm² s⁻¹). According to our measurements, the absorption coefficient is $\sim 20\%$. The thermal emissivity is $\varepsilon \approx 0.3$. The fluctuating temperature of the near-surface layer is described by the well-known expression

$$\delta T = \frac{2\alpha q}{\lambda} \left(\frac{\chi t}{\pi} \right)^{1/2}, \quad t < \tau, \quad (2)$$

where χ is the temperature conductivity and q is the laser radiation intensity in the focal spot. By equating the surface temperature $T_s = \bar{T} + \delta T$ to the boiling temperature, we find the variation in the boiling boundary with time:

$$\bar{T}(x, y) + \delta T(t) = T_b. \quad (3)$$

Because the laser energy in the boiling region is spent for vaporising the material, this results in a reduction in the energy heating the sample. The power \tilde{P} spent for heating is determined by the expression

$$\tilde{P} = \bar{P} \left[1 - \frac{1}{\tau \pi r_f^2} \int_{t_0}^{\tau} S_b(t) dt \right], \quad \tau > t > t_0, \quad (4)$$

where the surface S_b of boiling can be found from expression (3); t_0 is the instant of the onset of boiling; and $S_b(t_0) = 0$. The power \tilde{P} determines the average intensity appearing in Eqn (1):

$$\bar{q} = \frac{\tilde{P}}{\pi r_f^2}. \quad (5)$$

Therefore, the system of equations (1)–(5) describes the variation in the surface temperature following every pulse. With the knowledge of the dimensions of the melting and boiling regions, it is possible to determine approximately the mass of the melt removed per pulse and the reduction of the sample thickness h .

The regime of melt flow occurring upon irradiation by a laser beam with a large cross section and a moderate intensity has several specific features compared to the regimes discussed in the literature. In this case, a subsonic vapour outflow into the atmosphere is possible. An approximate condition for the subsonic-to-supersonic flow transition is the requirement that αq^* , where

$$q^* = c_s L \frac{p_a}{kT_b} m; \quad (6)$$

m is the mass of material vapour atoms; c_s is the sound speed in the metal vapour; p_a is the atmospheric pressure; and L is the specific sublimation energy [4]. For iron vapour, $q^* \approx 10^5 \text{ W cm}^{-2}$. If $\alpha q > q^*$, the vapour recoil pressure is proportional to the radiation intensity:

$$p = \alpha q c_s / L. \quad (7)$$

If $\alpha q < q^*$, the vapour recoil pressure is lower:

$$p = \left(\frac{\alpha q}{L}\right)^2 \frac{kT_b}{p_a m}. \quad (8)$$

For $\alpha q = q^*$, formulas (7) and (8) are equivalent.

Both these regimes can be realised in our conditions. When fusing is not through, under the vapour recoil pressure the melt will come into motion along the plate surface and the material will be ejected toward the beam. Such a region is small in the model of a thermally thin plate used here in use, and therefore we restrict ourselves to the process of forcing out the melt along the beam. This can occur when the plate is fused through. In our model, this may be the case for $r_m > h$, where r_m is the characteristic dimension of the melt region. When $S_b > 0$, the boiling region will acquire a momentum $p(\tau - t_0)S_b$ after pulsed irradiation. This will result in the increment in the velocity of the melt motion

$$\Delta V = \frac{p(\tau - t_0)}{\rho h},$$

where ρ is the density of the target material. During the interpulse period T_p , the liquid film will shift by a distance $\Delta V T_p = p(\tau - t_0)T_p / \rho h$. Taking into account (7), the expression for the film displacement during the interpulse period is

$$\Delta h = \frac{\alpha q c_s (\tau - t_0)}{L \rho h} T_p. \quad (9)$$

We assume that the film is disrupted when the total displacement caused by the action of pulses is equal to h . Finally, if the pulse radiation intensity is low but the pulse repetition rate is high, the melt removal is possible without the participation of vapour, owing to the melt flowing out by gravity, as was assumed in the remote cutting by cw laser radiation [2, 3]. If the maximum vertical dimension of the melt region reaches a critical value d_m^* , the entire melt region is removed from the plate, according to the model considered in Ref. [3]. As stated in Refs [2, 8], the value of d_m^* is given by the expressions

$$\frac{d_m^*}{R_c} = 4.4 \left(\frac{h}{R_c}\right)^{1/3}, \quad \frac{h}{R_c} < 0.75, \quad (10)$$

$$\frac{d_m^*}{R_c} = 4, \quad \frac{h}{R_c} > 0.75, \quad R_c = \left(\frac{\sigma_s}{\rho g}\right)^{1/2}, \quad (11)$$

where σ_s is the surface tension coefficient of the melt.

6. Results of numerical simulation and comparison with experiments

Fig. 1 shows the calculated shape of the cuts of a steel 50-mm high, 50-mm long plate of thickness $h = 0.5 \text{ mm}$ for different cutting speeds. One can see that the cut width decreases with increasing speed at a constant power. For specific speeds, the cut width fluctuates. The fluctuations are rather difficult to describe because of the finiteness of the spatial step in numerical calculations. For a near-critical speed, the cut begins not at the plate edge but at the point where the plate heating in the focal spot proves to be sufficient for cutting. The thickness of the thermal front is $\chi/V \sim 1 \text{ cm}$. As the laser beam comes within about this distance to the end of the plate, the temperature in the spot rises. As a consequence, the dimension of the melt region and the cut width also increase.

This boundary effect is also always observed in experiments. The initiation of cutting is sometimes accompanied by a periodic piercing of separate holes, but cutting stabilises after heating the plate. This result is also consistent with the experiment. Although this effect was not studied in detail, we believe that this instability is thermal in nature, since it is also observed in the remote cutting of steels with cw radiation [3]. The mechanism of this instability was qualitatively described in Ref. [3].

A quantitative comparison of the cut widths obtained numerically and experimentally is given in Table 1. Note that the cut width increases, for an invariable cutting speed, with the average power of laser radiation both in the experiment and in the calculations. The calculations performed for the focal spots of different dimension close to the experimental values showed that it had only a weak effect on the cutting parameters. This is also consistent with the experiment. To obtain a qualitative general picture of the remote cutting of steel plates, it is interesting to compare the calculated limiting cutting parameters with those obtained experimentally.

The formulation of the calculations corresponded to the experiment, i.e., the peak cutting speed was determined as a function of the average power in several cases: for a constant repetition rate $f = 100 \text{ Hz}$ and for a constant pulse energy $E_i = 2.2 \text{ J}$ (see Fig. 2). Referring to Fig. 2, the dependences in both cases are close. This is also indicative of the decisive role of the average power of laser radiation in remote cutting with a repetitively pulsed laser. The comparison of the calculations and the experiments was made for different absorption coefficients. The strongest correlation takes place for $\alpha = 20\%$, which is close to approximate experimental values. We note that the gravity-induced mass transfer would, in our circumstances, have given rise to a 5.2-mm wide cut, which was not observed either in the experiments or in the calculations.

Here, it is pertinent to compare the remote cutting of steel plates with repetitively pulsed and cw radiation [3] (see Fig. 3). Because these experiments were performed under different conditions, it makes sense to compare the limiting velocities for equal specific powers. The slope of the straight line drawn from the origin of coordinates to any point of the curves, $\tan \alpha = V_{cr}/(\bar{P}/h)$, is equal to the cut area per unit energy expended, i.e., to the cutting efficiency. One can see that the efficiency of a repetitively pulsed process is many times higher than that for the cw radiation. For $\bar{P}/h = 1 \text{ kW mm}^{-1}$, in particular, repetitively pulsed cutting efficiency is $6 \text{ mm}^2 \text{ kJ}^{-1}$ while the cw one is $2 \text{ mm}^2 \text{ kJ}^{-1}$. For

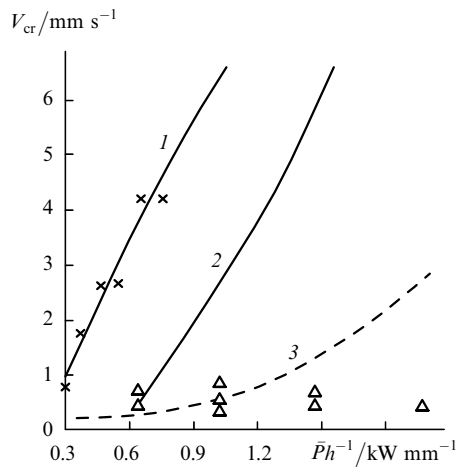


Figure 3. Experimental (symbols) and calculated (curves) maximum speed of cutting with a pulse-periodic (1, \times) and cw (2, 3, Δ) radiation for $f = 100$ Hz, $\alpha = 20\%$, and $\tau = 70$ μ s for $h = 0.5$ (1, 2, \times) and 2 mm (3). The experimental points labelled Δ were borrowed from Ref. [3].

a higher plate thickness ($h = 2$ mm), the efficiency of cw radiation cutting lowers to $0.5 \text{ mm}^2 \text{ kJ}^{-1}$.

7. Conclusions

Therefore, our study has shown the feasibility of regimes when additional energy expenditures for the material vaporisation in repetitively pulsed cutting assist in intensifying the melt removal from the interaction region. For this reason, the repetitively pulsed radiation cutting at a high off-duty ratio proves to be substantially more efficient than the cw radiation cutting. All qualitative dependences of the cutting parameters (cut width, critical velocity) on the experimental conditions (power, speed, degree of focusing, pulse duration) obtained in the calculations are consistent with the experimental ones. This confirms the validity of the mechanism of metal cutting considered above and the adequacy of the numerical model employed.

Acknowledgements. The authors thank A G Krasnyukov for proposing the subject of studies, his constant interest, and support of the work, and also the participants of the seminar conducted by him for helpful discussions. This work was partly supported by the Russian Foundation for Basic Research (Grant No. 00-02-16161) and the 'Gazprom' Co.

References

1. Krasnyukov A G, Kosyrev F K, Naumov V G, Shashkov V M *XII International Symposium on Gas and Chemical Lasers* (St. Petersburg, Russia, 1998)
2. Antonova G F, Gladush G G, Krasnyukov A G, Kosyrev F K, Sayapin V P *Teplofiz. Vys. Temp.* **37** 865 (1999) [*High Temp.* **37** 835 (1999)]
3. Antonova G F, Gladush G G, Krasnyukov A G, Kosyrev F K, Rodionov N B *Teplofiz. Vys. Temp.* **38** 501 (2000) [*High Temp.* **38** 477 (2000)]
4. Vedenov A A, Gladush G G *Fizicheskie Protssy pri Lazernoi Obrabotke Materialov* (Physical Processes in Laser Material Processing) (Moscow: Energoatomizdat, 1985)
5. Arutyunyan R V, Baranov V Yu, Bol'shov L A, et al. *Vozdeistvie Lazernogo Izlucheniya na Materialy* (Action of Laser Radiation on Materials) (Moscow: Nauka, 1989)

6. Markus S, Lowder J E, Mooney P L *J. Appl. Phys.* **47** 2966 (1976)
7. Gebhart B, Jaluria Y, Mahajan R, Sammakia B *Buoyancy-Induced Flows and Transport* (New York: Springer-Verlag, Hemisphere Publ., Harper&Row, 1988).
8. Likhanskii V V, Loboiko A I, Krasnyukov A G, Antonova G F, Sayapin V P *Kvantovaya Elektron.* **26** 139 (1999) [*Quantum Electron.* **29** 139 (1999)]